

## Review



# An Update on [<sup>18</sup>F]Fluoride PET Imaging for Atherosclerotic disease

Reeree Lee , Ju Won Seok

Department of Nuclear Medicine, Chung-Ang University Hospital, Seoul, Korea

## OPEN ACCESS

**Received:** Aug 12, 2020

**Revised:** Sep 2, 2020

**Accepted:** Sep 2, 2020

### Correspondence to

**Ju Won Seok**

Department of Nuclear Medicine, Chung-Ang University Hospital, 102 Heukseok-ro, Dongjak-gu, Seoul 06974, Korea.  
E-mail: joneseok@cau.ac.kr

Copyright © 2020 The Korean Society of Lipid and Atherosclerosis.

This is an Open Access article distributed under the terms of the Creative Commons Attribution Non-Commercial License (<https://creativecommons.org/licenses/by-nc/4.0/>) which permits unrestricted non-commercial use, distribution, and reproduction in any medium, provided the original work is properly cited.

### ORCID iDs

Reeree Lee

<https://orcid.org/0000-0001-8811-3699>

Ju Won Seok

<https://orcid.org/0000-0003-4107-2361>

### Funding

None.

### Conflict of Interest

The authors have no conflicts of interest to declare.

### Author Contributions

Conceptualization: Lee R, Seok JW; Writing - original draft: Lee R, Seok JW; Writing - review & editing: Lee R, Seok JW.

## ABSTRACT

Atherosclerosis is the leading cause of life-threatening morbidity and mortality, as the rupture of atherosclerotic plaques leads to critical atherothrombotic events such as myocardial infarction and ischemic stroke, which are the 2 most common causes of death worldwide. Vascular calcification is a complicated pathological process involved in atherosclerosis, and microcalcifications are presumed to increase the likelihood of plaque rupture. Despite many efforts to develop novel non-invasive diagnostic modalities, diagnostic techniques are still limited, especially before symptomatic presentation. From this point of view, vulnerable plaques are a direct target of atherosclerosis imaging. Anatomic imaging modalities have the limitation of only visualizing macroscopic structural changes, which occurs in later stages of disease, while molecular imaging modalities are able to detect microscopic processes and microcalcifications, which occur early in the disease process. Na[<sup>18</sup>F]-fluoride positron emission tomography/computed tomography could allow the early detection of plaque instability, which is deemed to be a primary goal in the prevention of cardiac or brain ischemic events, by quantifying the microcalcifications within vulnerable plaques and evaluating the atherosclerotic disease burden.

**Keywords:** Atherosclerosis; Sodium fluoride; Positron emission tomography; PET-CT

## INTRODUCTION

Atherosclerosis is the leading cause of life-threatening morbidity and mortality, as the rupture of atherosclerotic plaques leads to critical atherothrombotic events such as myocardial infarction and ischemic stroke, which are the 2 most common causes of death worldwide.<sup>1,2</sup>

Vascular calcification is an elaborate pathological process of atherosclerosis that is closely related to the beginning of atherosclerosis.<sup>3-5</sup> During the process of vascular calcification, “spotty” (micro)calcifications are a feature of high-risk plaque triggered by cell death and inflammation. While macrocalcifications are considered to reflect the healing process of chronic stable plaques, microcalcifications (calcium deposits smaller than 50 μm) are presumed to be an early marker of atherosclerosis, as they are the eventual components of macrocalcifications, and are associated with an increased propensity of plaque rupture

due to increased mechanical wall stress and a greater susceptibility of the plaque to microfractures.<sup>6,12</sup>

Despite many efforts to develop novel non-invasive diagnostic modalities, diagnostic techniques for atherosclerosis are still limited prior to ischemic manifestation. From this perspective, vulnerable plaques are a direct target of atherosclerosis imaging. Although recently used imaging modalities, including computed tomography (CT) angiography, magnetic resonance imaging, intravascular ultrasonography (IVUS), and optical coherence imaging focus on the composition of plaques (e.g., a thin fibrous cap, a lipid-rich necrotic core, neovascularization, intraplaque hemorrhage, and microcalcification) to identify vulnerable plaques,<sup>13,14</sup> they have the limitation of only visualizing macroscopic structural changes, which occur late in the course of disease. Unlike anatomic imaging, molecular imaging modalities can detect microscopic processes that occur early in the disease process.

Currently, the early detection of plaque instability has been deemed to be a primary goal in the prevention of cardiac or brain ischemic events. In contrast to anatomic imaging modalities, sodium fluoride (Na[<sup>18</sup>F]F) positron emission tomography (PET) for evaluating vascular osteogenesis in atherosclerotic plaques can detect early chemical changes. Employing this advanced imaging technique, it is possible to quantify the microcalcification within vulnerable plaques and to evaluate the atherosclerotic disease burden. The present review briefly discusses the molecular imaging modalities used for atherosclerosis and examines the available literature on the clinical application of Na[<sup>18</sup>F]F PET as a diagnostic tool of atherosclerosis.

## OVERVIEW OF MOLECULAR IMAGING FOR ATHEROSCLEROSIS

Atherosclerosis is an immunoinflammatory disease of the arterial wall, wherein a leaky and defective endothelium results in the infiltration of lipids and inflammatory cells within the intima. As the fibrous cap protecting the lipid core of a plaque becomes thin and ruptures, it can cause thrombus formation and lead to critical clinical events.<sup>15,16</sup> Owing to the complex and dynamic process of atherosclerotic plaques, they develop slowly and silently; hence they are often detected at a progressed stage.<sup>17</sup> In this regard, the early prevention and treatment of atherosclerosis are becoming of increasingly greater importance.

Although the aforementioned relatively recently developed techniques provide information on the composition of plaques, anatomical imaging modalities detect macroscopic structural changes, rather than microscopic changes, in vulnerable plaques.<sup>18-20</sup> To date, advances in molecular imaging have been adopted for non-invasive, *in vivo* detection of the biological signatures of atherosclerotic plaques. Various imaging targets and pertinent modalities for vulnerable plaque imaging are illustrated in **Fig. 1, 21** and summarized in the **Table 1.**<sup>22-40</sup> In particular, we focus on Na[<sup>18</sup>F]F PET/CT in the following section.

## NA[<sup>18</sup>F]F PET IMAGING OF MICROCALCIFICATIONS

### 1. Mechanism of Na[<sup>18</sup>F]F uptake in vascular microcalcifications

Initially, Na[<sup>18</sup>F]F PET was developed as a bone tracer, the activity of which is associated with high bone metabolism.<sup>42-44</sup> The mechanism of bony Na[<sup>18</sup>F]F uptake has been well studied.

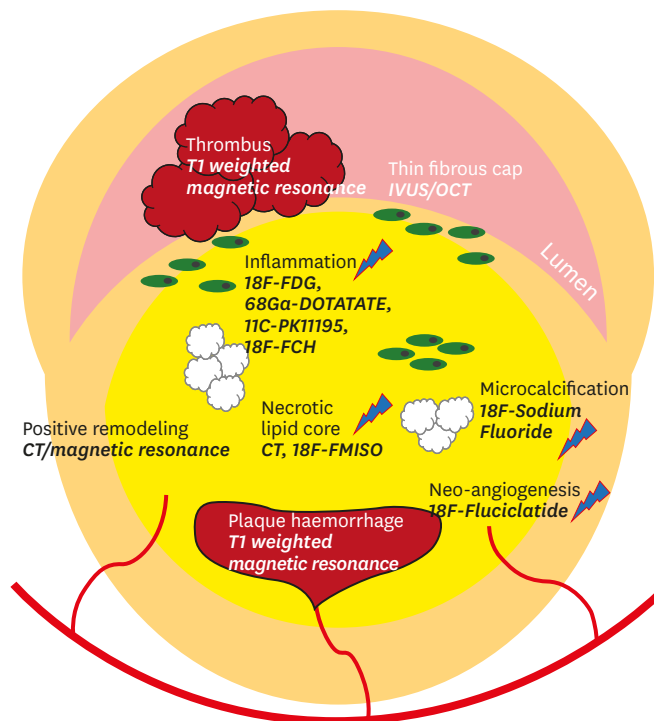


**Fig. 1.** Morphological and biological targets for atherosclerotic plaque imaging. Adopted from reference,<sup>21</sup> licensed under CC BY-NC-ND 4.0.

CT, computed tomography; IVUS, intravascular ultrasonography; OCT, optical coherence tomography; FDG, fluorodeoxyglucose; DOTATATE, DOTA-Tyr3-octreotate; FCH, fluorocholine; FMISO, fluoromisonidazole.

Na[<sup>18</sup>F]F diffuses into the bone extracellular fluid space through capillaries, and then fluoride ions are exchanged with hydroxyl ions of hydroxyapatite crystals on the bone surface to form fluoroapatite.<sup>42,44,45</sup> Therefore, the intensity of tracer uptake is mainly based on blood flow and the surface area of exposed hydroxyapatite.<sup>45</sup>

Irkle et al.<sup>46</sup> found that Na[<sup>18</sup>F]F binds only to the surface of macrocalcific deposits, and that Na[<sup>18</sup>F]F binding is increased in regions of microcalcifications. Since much of the hydroxyapatite in macroscopic deposits is internalized, it is not sufficient for Na[<sup>18</sup>F]F binding, and Na[<sup>18</sup>F]F is not capable of penetrating the crystalline mass.<sup>46,47</sup> Creager et al.<sup>45</sup> observed that Na[<sup>18</sup>F]F is taken up in areas of microcalcifications beyond the resolution of CT (200–500 μm in diameter)<sup>48,49</sup> and that higher Na[<sup>18</sup>F]F uptake was associated with the surface area of hydroxyapatite in their *in vitro* microcalcification model.<sup>45</sup> Since new calcium deposits undergo this microcalcification stage, successive examinations using Na[<sup>18</sup>F]F would document calcifying activity, enabling the detection of new ossification in the vasculature.

## 2. Early detection of atherosclerotic plaques

A series of studies have investigated the feasibility of Na[<sup>18</sup>F]F PET/CT to detect atherosclerotic plaques earlier than is possible using conventional CT. Researchers examined various segments of the vasculature, including the coronary arteries, aorta, iliac and femoral arteries, as well as the carotid arteries. In a retrospective study of 75 patients, Derlin et al.<sup>50</sup> found that almost all PET-positive sites (88%) were colocalized with calcifications detected by CT, but not many sites of calcification showed visible Na[<sup>18</sup>F]F uptake (12%). Li et al.<sup>51</sup> conducted a similar study in 61 patients and confirmed an association between Na[<sup>18</sup>F]F uptake and calcification in the same vascular territories, except for the abdominal aorta.

**Table 1.** Molecular imaging targets for atherosclerosis

Molecular probe	Target process	Results from clinical studies	Pitfalls
[ <sup>18</sup> F]FDG	Inflammation: glucose metabolism of inflammatory cells	<ul style="list-style-type: none"> <li>- Symptomatic culprit carotid plaques showed higher [<sup>18</sup>F]FDG uptake than non-culprit contralateral plaques.<sup>22,23</sup></li> <li>- Association between [<sup>18</sup>F]FDG uptake in carotid plaques and macrophage-specific antibody staining (CD68) of carotid endarterectomy specimens.<sup>24,25</sup></li> <li>- Association with the presence of recent or remote cardiovascular events.<sup>26-29</sup></li> <li>- Vascular [<sup>18</sup>F]FDG uptake in systemic inflammatory disease patients was higher than in healthy volunteers.<sup>30,31</sup></li> </ul>	<ul style="list-style-type: none"> <li>- Physiologic [<sup>18</sup>F]FDG signal in the myocardium hampering the epicardial coronary evaluation.</li> </ul>
<sup>68</sup> Ga or <sup>64</sup> Cu labeled DOTA-agents	Inflammation: SSTR of activated macrophage	<ul style="list-style-type: none"> <li>- Binding showed significant correlation with cardiovascular risk factors.<sup>32-35</sup></li> <li>- Non-colocalization of [<sup>18</sup>F]FDG and [<sup>68</sup>Ga]Ga-DOTATATE uptake in large arteries of atherosclerotic plaques was found.<sup>32</sup></li> <li>- Uptake was higher in culprit coronary and carotid lesions versus non-culprit arteries and exhibited superiority to differentiate high-risk from low-risk coronary atherosclerotic plaques over [<sup>18</sup>F]FDG PET uptake.<sup>36</sup></li> </ul>	<ul style="list-style-type: none"> <li>- Relatively inaccessible radiotracer</li> </ul>
[ <sup>18</sup> F]FCH	Inflammation: membrane metabolism of inflammatory cells	<ul style="list-style-type: none"> <li>- Uptake was not colocalized with CT visible calcification, and furthermore, none of the calcified lesions showed any [<sup>18</sup>F]FCH uptake.<sup>37</sup></li> <li>- A prospective clinical trial (NCT02640313) is currently underway, to see the efficiency of [<sup>18</sup>F]FCH PET/MRI in detecting intraplaque inflammation and identify vulnerable plaques that are prone to rupture in comparison to the stable ones.</li> </ul>	<ul style="list-style-type: none"> <li>- Insufficient validation as an atherosclerosis imaging</li> </ul>
<sup>11</sup> C-PK11195	Inflammation: TSPO of macrophages	<ul style="list-style-type: none"> <li>- Binding was correlated with immunostaining for CD68.<sup>38</sup></li> <li>- Uptake was observed in the arterial wall of symptomatic patients, but in none of the asymptomatic controls.<sup>39</sup></li> <li>- Uptake in culprit plaques from carotid endarterectomy tissue was higher compared with plaques from asymptomatic patients.<sup>40</sup></li> </ul>	<ul style="list-style-type: none"> <li>- Necessity of on-site cyclotron due to short half-life (20 min)</li> <li>- Non-specific binding</li> <li>- Low signal intensity</li> </ul>
[ <sup>18</sup> F]FMISO	Hypoxia	<ul style="list-style-type: none"> <li>- Symptomatic plaques showed higher [<sup>18</sup>F]FMISO uptake than contralateral asymptomatic plaques, and [<sup>18</sup>F]FMISO uptake correlated with higher [<sup>18</sup>F]FDG uptake.<sup>41</sup></li> </ul>	<ul style="list-style-type: none"> <li>- Higher cost</li> <li>- Insufficient validation as an atherosclerosis imaging</li> </ul>

FDG, fluorodeoxyglucose; DOTA, 1,4,7,10-tetraazacyclododecane-N,N',N'',N'''-tetraacetic acid-D-Phe1; SSTR, somatostatin receptor; FCH, fluorocholine; DOTATATE, DOTA-Tyr3-octreotate; TSPO, 18-kDa translocator protein; FMISO, fluoromisonidazole.

Fiz et al.<sup>52</sup> demonstrated that arterial wall uptake of Na[<sup>18</sup>F]F was inversely correlated with plaque density, suggesting that calcification in the early stage corresponds to the active phase of plaque formation. Quirce et al.<sup>53,54</sup> reported that symptomatic carotid plaques with low calcium content had higher Na[<sup>18</sup>F]F uptake than those with high levels of calcium deposits. Moreover, symptomatic carotid plaques exhibited higher Na[<sup>18</sup>F]F uptake than asymptomatic plaques.<sup>53,54</sup> In another retrospective study in patients with coronary artery disease (CAD), Na[<sup>18</sup>F]F uptake was slightly higher in partially calcified coronary plaques than in non-calcified and calcified coronary plaques.<sup>55</sup> These findings suggest that Na[<sup>18</sup>F]F signals can reveal the microcalcification process of plaques before they grow large enough to be distinguishable on CT. In addition, macrocalcifications lacking Na[<sup>18</sup>F]F uptake are no longer going through the active phase of mineralization.

### 3. Assessment of vulnerable, high-risk plaques

Vulnerable plaques and high-risk plaques are synonyms for describing plaques that are prone for thrombosis to occur. Detection of vulnerable plaques is worthwhile since doing so enables the timely trial of preventive measures against thromboembolic events.<sup>16</sup> In a prospective study conducted by Joshi et al.<sup>56</sup> in 40 patients who underwent Na[<sup>18</sup>F]F PET/CT after myocardial infarction, 37 (93%) patients showed higher Na[<sup>18</sup>F]F activity in the culprit plaque than in non-culprit plaques of coronary arteries or artery specimens. Furthermore, plaques with high Na[<sup>18</sup>F]F uptake exhibited high-risk morphological characteristics, including positive remodeling, microcalcification, and necrosis on IVUS.<sup>56</sup> In another prospective study in 26 patients who experienced cerebrovascular events (18 patients with culprit carotid stenosis and 8 control patients without a culprit lesion), the Na[<sup>18</sup>F]F binding of the excised culprit plaque was significantly higher than that of the contralateral asymptomatic plaque. Moreover,

Na[<sup>18</sup>F]F uptake showed a significant correlation with CT-derived high-risk plaque features and predicted cardiovascular risk (the ASSIGN score—assessing cardiovascular risk using SIGN guidelines to assign preventive treatment).<sup>47</sup> However, discordant results were reported in a prospective study in 20 patients with acute ischemic stroke. Neither Na[<sup>18</sup>F]F nor [<sup>18</sup>F] fluorodeoxyglucose (FDG) uptake showed a significant difference between culprit-positive and culprit-negative groups (10 patients in each group). This disagreement is thought to have occurred because both groups consisted of patients with recent stroke and moderate-to-severe carotid stenosis, of which the calcification burden is considerable.<sup>57</sup> Lee et al.<sup>58</sup> reported that patients with high-risk plaques assessed by IVUS and optical coherence tomography showed higher coronary Na[<sup>18</sup>F]F uptake than those with non-high-risk plaques in their prospective study of 51 patients with CAD. In 32 patients with CAD, Li et al.<sup>59</sup> also observed a relationship between coronary Na[<sup>18</sup>F]F uptake and high-risk plaque features on IVUS. In another recent study of *ex vivo* human coronary arteries, Youn et al.<sup>60</sup> demonstrated a correlation between coronary Na[<sup>18</sup>F]F uptake and histologically confirmed microcalcifications. These findings suggest that Na[<sup>18</sup>F]F PET allows the detection of vulnerable or culprit plaques in patients at increased cardio-cerebrovascular risk (**Fig. 2**).

#### 4. Relationship with cardiovascular risk factors

In an earlier retrospective study of 119 volunteers with and without aortic valve disease, individuals with enhanced coronary Na[<sup>18</sup>F]F uptake were more likely to have prior cardiovascular events, angina, and a higher Framingham Risk Score (FRS).<sup>6</sup> Fiz et al.<sup>61</sup> divided 78 patients who underwent Na[<sup>18</sup>F]F PET for evaluation of skeletal metastasis into 3 risk categories (high-, medium-, low-risk; HR, MR, LR, respectively) according to a simplified Framingham model. Na[<sup>18</sup>F]F activity in the thoracic aorta showed significant differences between HR and LR, between HR and MR, and between MR and LR. Thoracic Na[<sup>18</sup>F]F uptake was significantly correlated with a higher FRS, particularly in descending thoracic segments. They also assessed myocardial Na[<sup>18</sup>F]F deposition, as proposed by Beheshti et al.,<sup>62</sup> and suggested that global cardiac Na[<sup>18</sup>F]F uptake is an effective index of risk stratification.<sup>61</sup> In the prospective study conducted by Blomberg et al.<sup>63</sup> (the CAMONA study), a similar relationship was observed between thoracic aortic Na[<sup>18</sup>F]F uptake and a higher FRS, but not between [<sup>18</sup>F]FDG uptake and FRS, in 89 volunteers and 50 patients with angina. In another study in patients of the CAMONA study, the global tracer uptake value (GTUV) of [<sup>18</sup>F]FDG and Na[<sup>18</sup>F]F in the abdominal aorta was calculated and correlated with patients' age and FRS. The GTUV of Na[<sup>18</sup>F]F had a significant association with FRS and age, whereas [<sup>18</sup>F]FDG-derived GTUV showed no correlation with FRS in either healthy volunteers or patients with chest pain.<sup>64</sup>

In a recent study of 40 patients with suspected CAD, it was observed that the total Na[<sup>18</sup>F]F uptake of all lesions in the descending thoracic aorta was significantly correlated with higher hemoglobin A1c levels, while total lesion calcium deposition was associated with hypertension.<sup>65</sup> Since diabetes mellitus is thought to have a close association with vascular calcification,<sup>66</sup> it is suggested that Na[<sup>18</sup>F]F uptake indicates hyperglycemia-induced active calcification.<sup>65</sup> Rheumatoid arthritis (RA) is well recognized to be associated with an increased risk of cardiovascular disease.<sup>67</sup> Unlike the pilot study listed in the **Table 1**,<sup>30</sup> the average [<sup>18</sup>F]FDG uptake score showed no significant difference between 18 RA patients and 18 normal healthy controls in a prospective cross-sectional study. However, the Na[<sup>18</sup>F]F score was significantly higher in RA patients than in healthy controls. It was suggested that abdominal aortic molecular calcification is more likely to be increased in patients with RA than in healthy controls.<sup>68</sup>

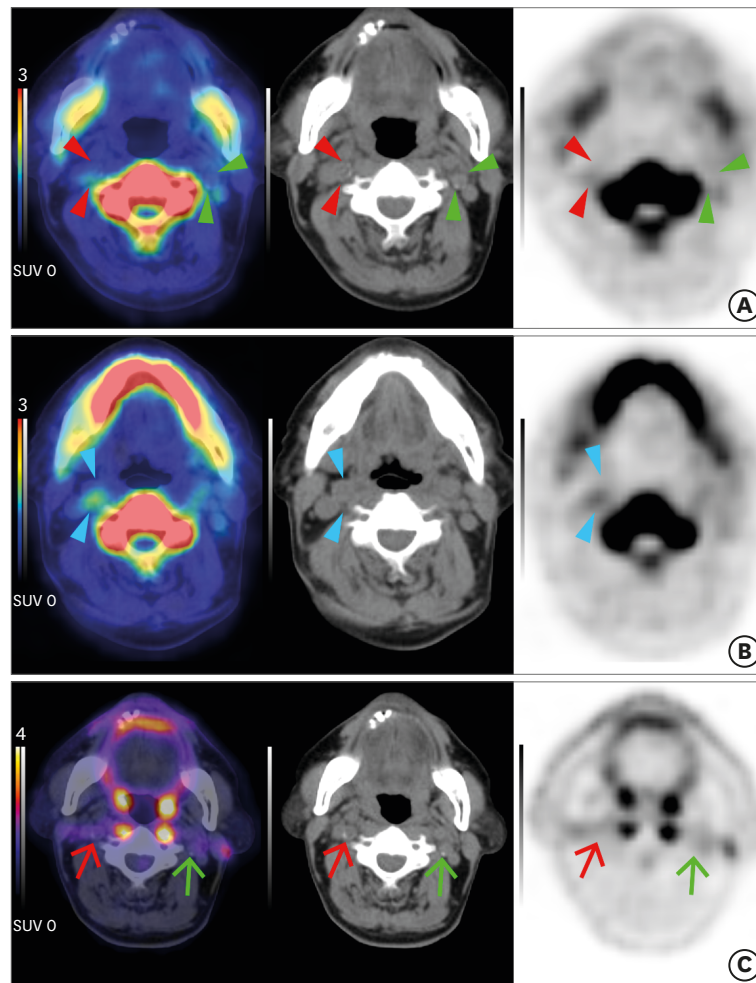


**Fig. 2.** Carotid plaques of a patient with acute stroke on Na[<sup>18</sup>F]F PET and [<sup>18</sup>F]FDG PET. A 77-year-old man with acute stroke in the right centrum semiovale, corona radiata, and superior frontal lobe due to total occlusion of the right proximal ICA. NaF (A, B) and FDG (C) PET/CT fusion (left), CT (middle), PET (right) axial images. (A) A low-attenuating culprit plaque showed focal Na[<sup>18</sup>F]F uptake in the right ICA on fusion PET/CT, CT, and PET images (red arrowheads). In contrast, left focal calcified asymptomatic carotid plaque did not exhibit Na[<sup>18</sup>F]F uptake (green arrowheads). (B) Note that more prominent Na[<sup>18</sup>F]F uptake was shown in the non-calcified portion of the culprit plaque (blue arrowheads). (C) In both culprit (red arrows) and non-culprit (green arrows) plaques, [<sup>18</sup>F] FDG uptake was not significantly increased. Images from our institution. Na[<sup>18</sup>F]F, sodium fluoride; PET, positron emission tomography; FDG, fluorodeoxyglucose; ICA, internal carotid artery; CT, computed tomography.

### 5. Beyond the aorta, coronary, and carotid arteries

Recently, several efforts have been made to evaluate Na[<sup>18</sup>F]F uptake in the pericardial fat and distal arteries, as well as in the coronary arteries, carotid arteries, and aorta. It has been demonstrated that an increased density of perivascular adipose tissue is associated with vascular inflammation, which spurs the development and progression of coronary atherosclerosis.<sup>69-71</sup> Kwiecinski et al.<sup>72</sup> sought to evaluate the relationship of an increased density of peri-coronary adipose tissue (PCAT) to Na[<sup>18</sup>F]F binding in 41 stable patients with high-risk coronary plaques. Na[<sup>18</sup>F]F uptake was well correlated with PCAT density, and PCAT density was higher in the plaques with Na[<sup>18</sup>F]F uptake than in those without Na[<sup>18</sup>F]F uptake.<sup>72</sup> In addition, the epicardial adipose tissue (EAT) has also attracted interest regarding its role in coronary atherosclerosis. Increased EAT volume measured on cardiac CT was shown to be related to CT-based coronary atherosclerosis.<sup>73,74</sup> In this regard, the association

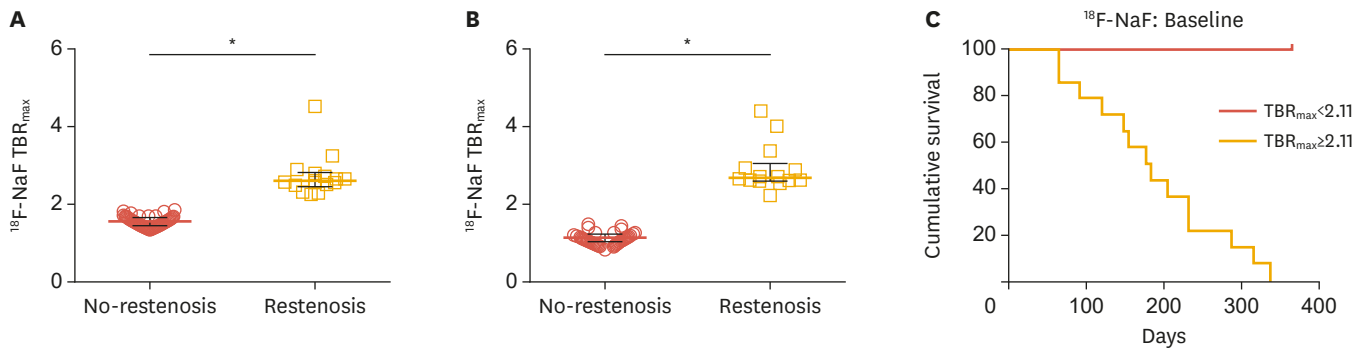


**Fig. 3.** Na[<sup>18</sup>F]F PET and restenosis in peripheral artery disease. Comparison of F-Na[<sup>18</sup>F]F uptake according to the restenosis status at 12 months, for both baseline (A) and post-PTA (B). Kaplan-Meier curves for Na[<sup>18</sup>F]F signal at baseline categorized according to TBRmax (C). Log-rank test *p*<0.001. Modified from reference,<sup>77</sup> licensed under CC BY 4.0.

Na[<sup>18</sup>F]F, sodium fluoride; PET, positron emission tomography; PTA, percutaneous transluminal angioplasty; TBRmax, target-to-background ratio maximum. \**p*<0.001.

between coronary arterial Na[<sup>18</sup>F]F uptake and EAT volume/density was evaluated. In 40 patients with more than 1 CT-detectable coronary plaque, perilesional EAT density was correlated with higher Na[<sup>18</sup>F]F uptake.<sup>75</sup> These results imply that Na[<sup>18</sup>F]F PET provides insights into the association between perivascular fat and atherosclerosis.

Na[<sup>18</sup>F]F signals have been assessed in peripheral arteries as well. In an early retrospective study in 409 cancer patients, linear Na[<sup>18</sup>F]F accumulation in the femoral artery showed correlations with age, hypertension, hypercholesterolemia, diabetes, history of smoking, prior cardiovascular events, and calcified plaque burden.<sup>76</sup> In a recent prospective study conducted by Chowdhury et al.,<sup>77</sup> 40 patients with symptomatic peripheral artery disease underwent baseline and 6-week follow-up [<sup>18</sup>F]FDG PET/CT and Na[<sup>18</sup>F]F PET/CT in the superficial femoral artery before receiving angioplasty. The baseline uptake of both [<sup>18</sup>F]FDG and Na[<sup>18</sup>F]F was higher in patients who developed restenosis within 12 months (*n*=14) after angioplasty, and this increase was shown on 6-week follow-up images as well. Uptake of both [<sup>18</sup>F]FDG and Na[<sup>18</sup>F]F was strongly predictive of 1-year vessel restenosis (Fig. 3).<sup>77</sup>

### 6. Clinical trials

The PREFFIR trial (NCT02278211) is a multi-center observational study aiming to determine the ability of Na[<sup>18</sup>F]F PET/CT to detect culprit plaques and predict disease recurrence or progression in 700 patients diagnosed with recent myocardial infarction and multi-vessel CAD.

Na[<sup>18</sup>F]F PET imaging has been used as an imaging endpoint in drug interventional clinical trials. Under the hypothesis that rosuvastatin improves plaque stability and decreases Na[<sup>18</sup>F]F plaque uptake, patients with Na[<sup>18</sup>F]F-positive plaques (coronary, aortic, or carotid) will be recruited and undergo Na[<sup>18</sup>F]F PET imaging at baseline and after treatment in the phase 4 ROPPET-NAF trial (NCT03233243). Another interventional clinical trial is utilizing baseline and follow-up Na[<sup>18</sup>F]F PET/CT imaging to quantify functional changes in coronary plaque burden and composition in patients treated with evolocumab in combination with statins (NCT03689946). In a recently terminated randomized, double-blind, placebo-controlled trial (NCT02110303), patients with multi-vessel CAD underwent coronary Na[<sup>18</sup>F]F PET/CT scanning to assess whether coronary Na[<sup>18</sup>F]F uptake could be used to identify patients with stable disease who respond favorably to ticagrelor.<sup>78</sup> Another randomized, double-blind, placebo-controlled trial (NCT02839044) sought to determine the effect of vitamin K on vascular calcification by using Na[<sup>18</sup>F]F PET/CT. In 33 patients with type 2 diabetes and known

cardiovascular disease, the study aimed to assess whether menaquinone supplementation decreased vascular calcification compared to placebo.<sup>79</sup>

### 7. Limitations

In spite of the outstanding sensitivity and specificity of Na[<sup>18</sup>F]F for atherosclerotic imaging, its limitations should be considered. The literature discussed herein is diverse in terms of the studied segments of the vasculature and methodology (e.g., quantification, analysis, acquisition protocol, etc.), making direct comparisons practically unfeasible. As arteries have relatively small volumes, they are susceptible to the partial volume effect. Therefore, motion artifacts resulting from respiratory/cardiac movements should be considered. Although blood-adjusted standardized uptake values have been most frequently used, various quantifying methods were used across studies, and there is no established standardization yet. Atherosclerosis is a systemic disease, and plaque rupture often occurs apart from the culprit lesion; hence, an assessment of the overall disease burden may provide more valuable information than a lesion-based approach in risk stratification.<sup>80,81</sup> In accordance with this rationale, the parameters derived by global arterial uptake measurements showed significant associations with cardiovascular risk factors.<sup>63,64,68,82-84</sup> The lack of long-term follow-up studies with the potential to elucidate the natural course and pathophysiology of microcalcifications in atheromas is another important consideration.

## CONCLUSION

In this review, we discussed the clinical implications of Na[<sup>18</sup>F]F PET for atherosclerosis imaging. [<sup>18</sup>F]F PET imaging allows non-invasive visualization of microcalcifications and early detection of vulnerable, high-risk plaques; therefore, it is expected to be used as an indication for earlier interventions. In addition, Na[<sup>18</sup>F]F PET holds promise as an assessment tool for accurate risk stratification, which will help to differentiate the patients who are most likely to benefit from early interventions and improve their outcomes. We have seen that Na[<sup>18</sup>F]F PET/CT can be used to evaluate pericardial/perilesional fat tissue or distal arteries, beyond the coronary/carotid arteries or aorta. Furthermore, investigation of the global disease burden was suggested as an appropriate methodology for the concept of systemic disease evaluation. With supplementation of the mentioned limitations and continued validation studies, Na[<sup>18</sup>F]F PET imaging has the potential to be a surrogate imaging biomarker for atherosclerosis.

## REFERENCES

1. Heron M. Deaths: leading causes for 2010. *Natl Vital Stat Rep* 2013;62:1-96.  
[PUBMED](#)
2. Benjamin EJ, Muntner P, Alonso A, Bittencourt MS, Callaway CW, Carson AP, et al. Heart disease and stroke statistics-2019 update: a report from the American Heart Association. *Circulation* 2019;139:e56-e528.  
[PUBMED](#) | [CROSSREF](#)
3. Demer LL, Tintut Y. Mineral exploration: search for the mechanism of vascular calcification and beyond: the 2003 Jeffrey M. Hoeg Award lecture. *Arterioscler Thromb Vasc Biol* 2003;23:1739-1743.  
[PUBMED](#) | [CROSSREF](#)
4. Johnson RC, Leopold JA, Loscalzo J. Vascular calcification: pathobiological mechanisms and clinical implications. *Circ Res* 2006;99:1044-1059.  
[PUBMED](#) | [CROSSREF](#)

5. Wu M, Rementer C, Giachelli CM. Vascular calcification: an update on mechanisms and challenges in treatment. *Calcif Tissue Int* 2013;93:365-373.  
[PUBMED](#) | [CROSSREF](#)
6. Dweck MR, Chow MWL, Joshi NV, Williams MC, Jones C, Fletcher AM, et al. Coronary arterial <sup>18</sup>F-sodium fluoride uptake: a novel marker of plaque biology. *J Am Coll Cardiol* 2012;59:1539-1548.  
[PUBMED](#) | [CROSSREF](#)
7. Kataoka Y, Wolski K, Uno K, Puri R, Tuzcu EM, Nissen SE, et al. Spotty calcification as a marker of accelerated progression of coronary atherosclerosis: insights from serial intravascular ultrasound. *J Am Coll Cardiol* 2012;59:1592-1597.  
[PUBMED](#) | [CROSSREF](#)
8. Vengrenyuk Y, Carlier S, Xanthos S, Cardoso L, Ganatos P, Virmani R, et al. A hypothesis for vulnerable plaque rupture due to stress-induced debonding around cellular microcalcifications in thin fibrous caps. *Proc Natl Acad Sci U S A* 2006;103:14678-14683.  
[PUBMED](#) | [CROSSREF](#)
9. Ehara S, Kobayashi Y, Yoshiyama M, Shimada K, Shimada Y, Fukuda D, et al. Spotty calcification typifies the culprit plaque in patients with acute myocardial infarction: an intravascular ultrasound study. *Circulation* 2004;110:3424-3429.  
[PUBMED](#) | [CROSSREF](#)
10. McEvoy JW, Blaha MJ, Defilippis AP, Budoff MJ, Nasir K, Blumenthal RS, et al. Coronary artery calcium progression: an important clinical measurement? A review of published reports. *J Am Coll Cardiol* 2010;56:1613-1622.  
[PUBMED](#) | [CROSSREF](#)
11. Ueda M. Clinical relevance of coronary artery calcification, as a risk factor for plaque rupture: viewpoint from pathology. *Clin Calcium* 2010;20:1656-1662.  
[PUBMED](#)
12. Kelly-Arnold A, Maldonado N, Laudier D, Aikawa E, Cardoso L, Weinbaum S. Revised microcalcification hypothesis for fibrous cap rupture in human coronary arteries. *Proc Natl Acad Sci U S A* 2013;110:10741-10746.  
[PUBMED](#) | [CROSSREF](#)
13. Osborn EA, Jaffer FA. Imaging atherosclerosis and risk of plaque rupture. *Curr Atheroscler Rep* 2013;15:359.  
[PUBMED](#) | [CROSSREF](#)
14. Moghbel M, Al-Zaghal A, Werner TJ, Constantinescu CM, Høilund-Carlsen PF, Alavi A. The role of PET in evaluating atherosclerosis: a critical review. *Semin Nucl Med* 2018;48:488-497.  
[PUBMED](#) | [CROSSREF](#)
15. Falk E. Pathogenesis of atherosclerosis. *J Am Coll Cardiol* 2006;47:C7-C12.  
[PUBMED](#) | [CROSSREF](#)
16. Schaar JA, Muller JE, Falk E, Virmani R, Fuster V, Serruys PW, et al. Terminology for high-risk and vulnerable coronary artery plaques. Report of a meeting on the vulnerable plaque, June 17 and 18, 2003, Santorini, Greece. *Eur Heart J* 2004;25:1077-1082.  
[PUBMED](#) | [CROSSREF](#)
17. Tarkin JM, Joshi FR, Rudd JH. PET imaging of inflammation in atherosclerosis. *Nat Rev Cardiol* 2014;11:443-457.  
[PUBMED](#) | [CROSSREF](#)
18. Motoyama S, Sarai M, Harigaya H, Anno H, Inoue K, Hara T, et al. Computed tomographic angiography characteristics of atherosclerotic plaques subsequently resulting in acute coronary syndrome. *J Am Coll Cardiol* 2009;54:49-57.  
[PUBMED](#) | [CROSSREF](#)
19. Cai J, Hatsukami TS, Ferguson MS, Kerwin WS, Saam T, Chu B, et al. *In vivo* quantitative measurement of intact fibrous cap and lipid-rich necrotic core size in atherosclerotic carotid plaque: comparison of high-resolution, contrast-enhanced magnetic resonance imaging and histology. *Circulation* 2005;112:3437-3444.  
[PUBMED](#) | [CROSSREF](#)
20. Obaid DR, Calvert PA, Gopalan D, Parker RA, Hoole SP, West NE, et al. Atherosclerotic plaque composition and classification identified by coronary computed tomography: assessment of computed tomography-generated plaque maps compared with virtual histology intravascular ultrasound and histology. *Circ Cardiovasc Imaging* 2013;6:655-664.  
[PUBMED](#) | [CROSSREF](#)
21. Andrews JPM, Fayad ZA, Dweck MR. New methods to image unstable atherosclerotic plaques. *Atherosclerosis* 2018;272:118-128.  
[PUBMED](#) | [CROSSREF](#)
22. Rudd JHF, Warburton EA, Fryer TD, Jones HA, Clark JC, Antoun N, et al. Imaging atherosclerotic plaque inflammation with [<sup>18</sup>F]-fluorodeoxyglucose positron emission tomography. *Circulation* 2002;105:2708-2711.  
[PUBMED](#) | [CROSSREF](#)

23. Kim JM, Lee ES, Park KY, Seok JW, Kwon OS. Analysis of <sup>18</sup>F-fluorodeoxyglucose and <sup>18</sup>F-fluoride positron emission tomography in Korean stroke patients with carotid atherosclerosis. *J Lipid Atheroscler* 2019;8:232-241.  
[PUBMED](#) | [CROSSREF](#)
24. Tawakol A, Migrino RQ, Bashian GG, Bedri S, Vermeylen D, Cury RC, et al. *In vivo* <sup>18</sup>F-fluorodeoxyglucose positron emission tomography imaging provides a noninvasive measure of carotid plaque inflammation in patients. *J Am Coll Cardiol* 2006;48:1818-1824.  
[PUBMED](#) | [CROSSREF](#)
25. Graebe M, Pedersen SF, Borgwardt L, Højgaard L, Sillesen H, Kjaer A. Molecular pathology in vulnerable carotid plaques: correlation with [18]-fluorodeoxyglucose positron emission tomography (FDG-PET). *Eur J Vasc Endovasc Surg* 2009;37:714-721.  
[PUBMED](#) | [CROSSREF](#)
26. Paulmier B, Duet M, Khayat R, Pierquet-Ghazzar N, Laissy JP, Maunoury C, et al. Arterial wall uptake of fluorodeoxyglucose on PET imaging in stable cancer disease patients indicates higher risk for cardiovascular events. *J Nucl Cardiol* 2008;15:209-217.  
[PUBMED](#) | [CROSSREF](#)
27. Figueroa AL, Subramanian SS, Cury RC, Truong QA, Gardecki JA, Tearney GJ, et al. Distribution of inflammation within carotid atherosclerotic plaques with high-risk morphological features: a comparison between positron emission tomography activity, plaque morphology, and histopathology. *Circ Cardiovasc Imaging* 2012;5:69-77.  
[PUBMED](#) | [CROSSREF](#)
28. Figueroa AL, Abdelbaky A, Truong QA, Corsini E, MacNabb MH, Lavender ZR, et al. Measurement of arterial activity on routine FDG PET/CT images improves prediction of risk of future CV events. *JACC Cardiovasc Imaging* 2013;6:1250-1259.  
[PUBMED](#) | [CROSSREF](#)
29. Kelly PJ, Camps-Renom P, Giannotti N, Martí-Fàbregas J, Murphy S, McNulty J, et al. Carotid plaque inflammation imaged by <sup>18</sup>F-fluorodeoxyglucose positron emission tomography and risk of early recurrent stroke. *Stroke* 2019;50:1766-1773.  
[PUBMED](#) | [CROSSREF](#)
30. Rose S, Sheth NH, Baker JF, Ogdie A, Raper A, Saboury B, et al. A comparison of vascular inflammation in psoriasis, rheumatoid arthritis, and healthy subjects by FDG-PET/CT: a pilot study. *Am J Cardiovasc Dis* 2013;3:273-278.  
[PUBMED](#)
31. Naik HB, Natarajan B, Stansky E, Ahlman MA, Teague H, Salahuddin T, et al. Severity of psoriasis associates with aortic vascular inflammation detected by FDG PET/CT and neutrophil activation in a prospective observational study. *Arterioscler Thromb Vasc Biol* 2015;35:2667-2676.  
[PUBMED](#) | [CROSSREF](#)
32. Li X, Samnick S, Lapa C, Israel I, Buck AK, Kreissl MC, et al. <sup>68</sup>Ga-DOTATATE PET/CT for the detection of inflammation of large arteries: correlation with <sup>18</sup>F-FDG, calcium burden and risk factors. *EJNMMI Res* 2012;2:52.  
[PUBMED](#) | [CROSSREF](#)
33. Malmberg C, Ripa RS, Johnbeck CB, Knigge U, Langer SW, Mortensen J, et al. <sup>64</sup>Cu-DOTATATE for noninvasive assessment of atherosclerosis in large arteries and its correlation with risk factors: head-to-head comparison with <sup>68</sup>Ga-DOTATOC in 60 patients. *J Nucl Med* 2015;56:1895-1900.  
[PUBMED](#) | [CROSSREF](#)
34. Rominger A, Saam T, Vogl E, Ubleis C, la Fougère C, Förster S, et al. *In vivo* imaging of macrophage activity in the coronary arteries using <sup>68</sup>Ga-DOTATATE PET/CT: correlation with coronary calcium burden and risk factors. *J Nucl Med* 2010;51:193-197.  
[PUBMED](#) | [CROSSREF](#)
35. Lee R, Kim J, Paeng JC, Byun JW, Cheon GJ, Lee DS, et al. Measurement of <sup>68</sup>Ga-DOTATOC uptake in the thoracic aorta and its correlation with cardiovascular risk. *Nucl Med Mol Imaging* 2018;52:279-286.  
[PUBMED](#) | [CROSSREF](#)
36. Tarkin JM, Joshi FR, Evans NR, Chowdhury MM, Figg NL, Shah AV, et al. Detection of atherosclerotic inflammation by <sup>68</sup>Ga-DOTATATE PET compared to [<sup>18</sup>F]FDG PET imaging. *J Am Coll Cardiol* 2017;69:1774-1791.  
[PUBMED](#) | [CROSSREF](#)
37. Bucerius J, Schmaljohann J, Böhm I, Palmedo H, Gohlke S, Tiemann K, et al. Feasibility of <sup>18</sup>F-fluoromethylcholine PET/CT for imaging of vessel wall alterations in humans--first results. *Eur J Nucl Med Mol Imaging* 2008;35:815-820.  
[PUBMED](#) | [CROSSREF](#)

38. Fujimura Y, Hwang PM, Trout Iii H, Kozloff L, Imaizumi M, Innis RB, et al. Increased peripheral benzodiazepine receptors in arterial plaque of patients with atherosclerosis: an autoradiographic study with [(3)H]PK 11195. *Atherosclerosis* 2008;201:108-111.  
[PUBMED](#) | [CROSSREF](#)
39. Pugliese F, Gaemperli O, Kinderlerer AR, Lamare F, Shalhoub J, Davies AH, et al. Imaging of vascular inflammation with [11C]-PK11195 and positron emission tomography/computed tomography angiography. *J Am Coll Cardiol* 2010;56:653-661.  
[PUBMED](#) | [CROSSREF](#)
40. Gaemperli O, Shalhoub J, Owen DR, Lamare F, Johansson S, Fouladi N, et al. Imaging intraplaque inflammation in carotid atherosclerosis with 11C-PK11195 positron emission tomography/computed tomography. *Eur Heart J* 2012;33:1902-1910.  
[PUBMED](#) | [CROSSREF](#)
41. Joshi FR, Manavaki R, Fryer TD, Figg NL, Sluimer JC, Aigbirhio FI, et al. Vascular imaging with <sup>18</sup>F-fluorodeoxyglucose positron emission tomography is influenced by hypoxia. *J Am Coll Cardiol* 2017;69:1873-1874.  
[PUBMED](#) | [CROSSREF](#)
42. Blau M, Ganatra R, Bender MA. 18 F-fluoride for bone imaging. *Semin Nucl Med* 1972;2:31-37.  
[PUBMED](#) | [CROSSREF](#)
43. Hawkins RA, Choi Y, Huang SC, Hoh CK, Dahlbom M, Schiepers C, et al. Evaluation of the skeletal kinetics of fluorine-18-fluoride ion with PET. *J Nucl Med* 1992;33:633-642.  
[PUBMED](#)
44. Czernin J, Satyamurthy N, Schiepers C. Molecular mechanisms of bone <sup>18</sup>F-NaF deposition. *J Nucl Med* 2010;51:1826-1829.  
[PUBMED](#) | [CROSSREF](#)
45. Creager MD, Hohl T, Hutcheson JD, Moss AJ, Schlotter F, Blaser MC, et al. <sup>18</sup>F-fluoride signal amplification identifies microcalcifications associated with atherosclerotic plaque instability in positron emission tomography/computed tomography images. *Circ Cardiovasc Imaging* 2019;12:e007835.  
[PUBMED](#) | [CROSSREF](#)
46. Irkle A, Vesey AT, Lewis DY, Skepper JN, Bird JL, Dweck MR, et al. Identifying active vascular microcalcification by (18)F-sodium fluoride positron emission tomography. *Nat Commun* 2015;6:7495.  
[PUBMED](#) | [CROSSREF](#)
47. Vesey AT, Jenkins WSA, Irkle A, Moss A, Sng G, Forsythe RO, et al. <sup>18</sup>F-fluoride and <sup>18</sup>F-fluorodeoxyglucose positron emission tomography after transient ischemic attack or minor ischemic stroke: case-control study. *Circ Cardiovasc Imaging* 2017;10:e004976.  
[PUBMED](#) | [CROSSREF](#)
48. Stary HC. Natural history of calcium deposits in atherosclerosis progression and regression. *Z Kardiol* 2000;89 Suppl 2:28-35.  
[PUBMED](#) | [CROSSREF](#)
49. Ritman EL. Small-animal CT - its difference from, and impact on, clinical CT. *Nucl Instrum Methods Phys Res A* 2007;580:968-970.  
[PUBMED](#) | [CROSSREF](#)
50. Derlin T, Richter U, Bannas P, Begemann P, Buchert R, Mester J, et al. Feasibility of <sup>18</sup>F-sodium fluoride PET/CT for imaging of atherosclerotic plaque. *J Nucl Med* 2010;51:862-865.  
[PUBMED](#) | [CROSSREF](#)
51. Li Y, Berenji GR, Shaba WF, Tafti B, Yevdayev E, Dadparvar S. Association of vascular fluoride uptake with vascular calcification and coronary artery disease. *Nucl Med Commun* 2012;33:14-20.  
[PUBMED](#) | [CROSSREF](#)
52. Fiz F, Morbelli S, Piccardo A, Bauckneht M, Ferrarazzo G, Pestarino E, et al. <sup>18</sup>F-NaF uptake by atherosclerotic plaque on PET/CT imaging: inverse correlation between calcification density and mineral metabolic activity. *J Nucl Med* 2015;56:1019-1023.  
[PUBMED](#) | [CROSSREF](#)
53. Quirce R, Martínez-Rodríguez I, De Arcocha Torres M, Jiménez-Bonilla JF, Banzo I, Rebollo M, et al. Contribution of <sup>18</sup>F-sodium fluoride PET/CT to the study of the carotid atheroma calcification. *Rev Esp Med Nucl Imagen Mol* 2013;32:22-25.  
[PUBMED](#)
54. Quirce R, Martínez-Rodríguez I, Banzo I, Jiménez-Bonilla J, Martínez-Amador N, Ibáñez-Bravo S, et al. New insight of functional molecular imaging into the atheroma biology: <sup>18</sup>F-NaF and <sup>18</sup>F-FDG in symptomatic and asymptomatic carotid plaques after recent CVA. Preliminary results. *Clin Physiol Funct Imaging* 2016;36:499-503.  
[PUBMED](#) | [CROSSREF](#)

55. Kitagawa T, Yamamoto H, Toshimitsu S, Sasaki K, Senoo A, Kubo Y, et al. <sup>18</sup>F-sodium fluoride positron emission tomography for molecular imaging of coronary atherosclerosis based on computed tomography analysis. *Atherosclerosis* 2017;263:385-392.  
[PUBMED](#) | [CROSSREF](#)
56. Joshi NV, Vesey AT, Williams MC, Shah ASV, Calvert PA, Craighead FHM, et al. <sup>18</sup>F-fluoride positron emission tomography for identification of ruptured and high-risk coronary atherosclerotic plaques: a prospective clinical trial. *Lancet* 2014;383:705-713.  
[PUBMED](#) | [CROSSREF](#)
57. Kim JM, Lee ES, Park KY, Seok JW, Kwon OS. Comparison of [<sup>18</sup>F]-FDG and [<sup>18</sup>F]-NaF positron emission tomography on culprit carotid atherosclerosis: a prospective study. *JACC Cardiovasc Imaging* 2019;12:370-372.  
[PUBMED](#) | [CROSSREF](#)
58. Lee JM, Bang JI, Koo BK, Hwang D, Park J, Zhang J, et al. Clinical relevance of <sup>18</sup>F-sodium fluoride positron-emission tomography in noninvasive identification of high-risk plaque in patients with coronary artery disease. *Circ Cardiovasc Imaging* 2017;10:e006704.  
[PUBMED](#) | [CROSSREF](#)
59. Li L, Li X, Jia Y, Fan J, Wang H, Fan C, et al. Sodium-fluoride PET-CT for the non-invasive evaluation of coronary plaques in symptomatic patients with coronary artery disease: a cross-correlation study with intravascular ultrasound. *Eur J Nucl Med Mol Imaging* 2018;45:2181-2189.  
[PUBMED](#) | [CROSSREF](#)
60. Youn T, Al'Aref SJ, Narula N, Salvatore S, Pisapia D, Dweck MR, et al. <sup>18</sup>F-sodium fluoride positron emission tomography/computed tomography in *ex vivo* human coronary arteries with histological correlation. *Arterioscler Thromb Vasc Biol* 2020;40:404-411.  
[PUBMED](#) | [CROSSREF](#)
61. Fiz F, Morbelli S, Bauckneht M, Piccardo A, Ferrarazzo G, Nieri A, et al. Correlation between thoracic aorta <sup>18</sup>F-natrium fluoride uptake and cardiovascular risk. *World J Radiol* 2016;8:82-89.  
[PUBMED](#) | [CROSSREF](#)
62. Beheshti M, Saboury B, Mehta NN, Torigian DA, Werner T, Mohler E, et al. Detection and global quantification of cardiovascular molecular calcification by fluoro18-fluoride positron emission tomography/computed tomography--a novel concept. *Hell J Nucl Med* 2011;14:114-120.  
[PUBMED](#)
63. Blomberg BA, de Jong PA, Thomassen A, Lam MGE, Vach W, Olsen MH, et al. Thoracic aorta calcification but not inflammation is associated with increased cardiovascular disease risk: results of the CAMONA study. *Eur J Nucl Med Mol Imaging* 2017;44:249-258.  
[PUBMED](#) | [CROSSREF](#)
64. Arani LS, Gharavi MH, Zadeh MZ, Raynor WY, Seraj SM, Constantinescu CM, et al. Association between age, uptake of <sup>18</sup>F-fluorodeoxyglucose and of <sup>18</sup>F-sodium fluoride, as cardiovascular risk factors in the abdominal aorta. *Hell J Nucl Med* 2019;22:14-19.  
[PUBMED](#)
65. Ryoo HG, Paeng JC, Koo BK, Cheon GJ, Lee DS, Kang KW. Clinical implication of <sup>18</sup>F-NaF PET/computed tomography indexes of aortic calcification in coronary artery disease patients: correlations with cardiovascular risk factors. *Nucl Med Commun* 2020;41:58-64.  
[PUBMED](#) | [CROSSREF](#)
66. Yahagi K, Kolodgie FD, Lutter C, Mori H, Romero ME, Finn AV, et al. Pathology of human coronary and carotid artery atherosclerosis and vascular calcification in diabetes mellitus. *Arterioscler Thromb Vasc Biol* 2017;37:191-204.  
[PUBMED](#) | [CROSSREF](#)
67. Meyer PW, Anderson R, Ker JA, Ally MT. Rheumatoid arthritis and risk of cardiovascular disease. *Cardiovasc J Afr* 2018;29:317-321.  
[PUBMED](#) | [CROSSREF](#)
68. Seraj SM, Raynor WY, Revheim ME, Al-Zaghal A, Zadeh MZ, Arani LS, et al. Assessing the feasibility of NaF-PET/CT versus FDG-PET/CT to detect abdominal aortic calcification or inflammation in rheumatoid arthritis patients. *Ann Nucl Med* 2020;34:424-431.  
[PUBMED](#) | [CROSSREF](#)
69. Hedgire S, Baliyan V, Zucker EJ, Bittner DO, Staziaki PV, Takx RAP, et al. Perivascular epicardial fat stranding at coronary CT angiography: a marker of acute plaque rupture and spontaneous coronary artery dissection. *Radiology* 2018;287:808-815.  
[PUBMED](#) | [CROSSREF](#)

70. Margaritis M, Antonopoulos AS, Digby J, Lee R, Reilly S, Coutinho P, et al. Interactions between vascular wall and perivascular adipose tissue reveal novel roles for adiponectin in the regulation of endothelial nitric oxide synthase function in human vessels. *Circulation* 2013;127:2209-2221.  
[PUBMED](#) | [CROSSREF](#)
71. Marwan M, Hell M, Schuhbäck A, Gauss S, Bittner D, Pflederer T, et al. CT attenuation of pericoronary adipose tissue in normal versus atherosclerotic coronary segments as defined by intravascular ultrasound. *J Comput Assist Tomogr* 2017;41:762-767.  
[PUBMED](#) | [CROSSREF](#)
72. Kwiecinski J, Dey D, Cadet S, Lee SE, Otaki Y, Huynh PT, et al. Peri-coronary adipose tissue density is associated with <sup>18</sup>F-sodium fluoride coronary uptake in stable patients with high-risk plaques. *JACC Cardiovasc Imaging* 2019;12:2000-2010.  
[PUBMED](#) | [CROSSREF](#)
73. Yerramasu A, Dey D, Venuraju S, Anand DV, Atwal S, Corder R, et al. Increased volume of epicardial fat is an independent risk factor for accelerated progression of sub-clinical coronary atherosclerosis. *Atherosclerosis* 2012;220:223-230.  
[PUBMED](#) | [CROSSREF](#)
74. Oka T, Yamamoto H, Ohashi N, Kitagawa T, Kunita E, Utsunomiya H, et al. Association between epicardial adipose tissue volume and characteristics of non-calcified plaques assessed by coronary computed tomographic angiography. *Int J Cardiol* 2012;161:45-49.  
[PUBMED](#) | [CROSSREF](#)
75. Kitagawa T, Nakamoto Y, Fujii Y, Sasaki K, Tatsugami F, Awai K, et al. Relationship between coronary arterial <sup>18</sup>F-sodium fluoride uptake and epicardial adipose tissue analyzed using computed tomography. *Eur J Nucl Med Mol Imaging* 2020;47:1746-1756.  
[PUBMED](#) | [CROSSREF](#)
76. Janssen T, Bannas P, Herrmann J, Veldhoen S, Busch JD, Treszl A, et al. Association of linear <sup>18</sup>F-sodium fluoride accumulation in femoral arteries as a measure of diffuse calcification with cardiovascular risk factors: a PET/CT study. *J Nucl Cardiol* 2013;20:569-577.  
[PUBMED](#) | [CROSSREF](#)
77. Chowdhury MM, Tarkin JM, Albaghdadi MS, Evans NR, Le EPV, Berrett TB, et al. Vascular positron emission tomography and restenosis in symptomatic peripheral arterial disease: a prospective clinical study. *JACC Cardiovasc Imaging* 2020;13:1008-1017.  
[PUBMED](#) | [CROSSREF](#)
78. Moss AJ, Dweck MR, Doris MK, Andrews JPM, Bing R, Forsythe RO, et al. Ticagrelor to reduce myocardial injury in patients with high-risk coronary artery plaque. *JACC Cardiovasc Imaging* 2020;13:1549-1560.  
[PUBMED](#) | [CROSSREF](#)
79. Zwakenberg SR, de Jong PA, Bartstra JW, van Asperen R, Westerink J, de Valk H, et al. The effect of menaquinone-7 supplementation on vascular calcification in patients with diabetes: a randomized, double-blind, placebo-controlled trial. *Am J Clin Nutr* 2019;110:883-890.  
[PUBMED](#) | [CROSSREF](#)
80. Alavi A, Werner TJ, Høilund-Carlsen PF. PET-based imaging to detect and characterize cardiovascular disorders: unavoidable path for the foreseeable future. *J Nucl Cardiol* 2018;25:203-207.  
[PUBMED](#) | [CROSSREF](#)
81. Alavi A, Werner TJ, Høilund-Carlsen PF. What can be and what cannot be accomplished with PET to detect and characterize atherosclerotic plaques. *J Nucl Cardiol* 2018;25:2012-2015.  
[PUBMED](#) | [CROSSREF](#)
82. Blomberg BA, Thomassen A, de Jong PA, Lam MGE, Diederichsen ACP, Olsen MH, et al. Coronary fluorine-18-sodium fluoride uptake is increased in healthy adults with an unfavorable cardiovascular risk profile: results from the CAMONA study. *Nucl Med Commun* 2017;38:1007-1014.  
[PUBMED](#) | [CROSSREF](#)
83. Sorci O, Batzdorf AS, Mayer M, Rhodes S, Peng M, Jankelovits AR, et al. <sup>18</sup>F-sodium fluoride PET/CT provides prognostic clarity compared to calcium and Framingham risk scoring when addressing whole-heart arterial calcification. *Eur J Nucl Med Mol Imaging* 2020;47:1678-1687.  
[PUBMED](#) | [CROSSREF](#)
84. Kwiecinski J, Cadet S, Daghem M, Lassen ML, Dey D, Dweck MR, et al. Whole-vessel coronary <sup>18</sup>F-sodium fluoride PET for assessment of the global coronary microcalcification burden. *Eur J Nucl Med Mol Imaging* 2020;47:1736-1745.  
[PUBMED](#) | [CROSSREF](#)